JIHEN LOUKIL[1,*], NABIL DERBEL[2]

J. Electrical Systems 15-3 (2019): 459-479

Regular paper

Control Strategy For a Photovoltaic/Lead-Acid Batteries Energy Production System

For an efficiently use of the photovoltaic energy as well as for the energy supply optimization, an effective control strategy is highly needed. Therefore, this paper proposes an intelligent control method for an energy generation system composed by a solar panel, a DC-DC converters and a pack of lead-acid batteries. Firstly, a dynamic modeling of different electrical energy components has been carried out. Then an online Elman Neural Network (ENN) based controller has been designed and developed in order to perform the tracking of the optimal operating point of the solar source. Moreover, a Fuzzy Logic Controller (FLC) has been adopted for the adjustment of the PI parameters of the lead acid batteries controllers. Simulation results obtained in the Matlab/Simulink environment confirm the efficiently of the adopted control scheme.

Keywords: Photovoltaic system; DC-DC converter; Lead acid battery; DC bus; Control; Simulation; Maximum Power Point Tracker (MPPT); Elman Neural Network (ENN); Energy Management System; Fuzzy Logic Controller.
Article history: Received 25 December 2018, Accepted 10 May 2019

1. Introduction

Unit Electrical power production systems have being asked to meet the accelerated growth demand of electricity with high quality and uninterrupted supply. In fact, the current worldwide consumption capacity has been estimated to be about 20 terawatt hours. For many years, this requirement has been achieved by the use of fossil fuels thanks to their flexibility of transport and storage. But, with an aggressive development of efficient and new technologies, the worldwide electricity demand has been increasing at a faster pace than overall energy consumption. At the same time, Coal which has been considered as the dominant source of electricity generation in the world produces by its burning an average 1000 g of CO_2 emission for every KWh of generated electricity. Therefore, the environmental concerns over the use of fossil fuels and their resource constraints, combined with energy security concerns, have been spurred great interest in generating electric energy from renewable sources. In fact, nowadays, wind power and solar photovoltaic (PV) have been considered as the most abundant and potentially readily available. They have received a considerable attention thanks to their several benefits. The sun, seen as a promising source of energy, has been occupied the center of interest for several research teams in the world for several decades. It is considered as an inexhaustible mine of energy with the greatest potential for development compared with other sources. It presents the advantages of durability, cleanness, and zero dioxide emissions that endanger human health and nature. Many countries in the world have been fully engaged in the energy transition strategy by adopting a proactive energy control policy to encourage photovoltaic renewable energy development [1], [2], [3]. Solar energy sources have a problem in terms of power generation due to their unpredictable and intermittent availability.

[1] Phd in University of Sfax, Sfax Engineering School, Control & Energy Management Laboratory (CEMLab), Sfax, Tunisia. E-mail:jihen.loukil@gmail.com
[2] Professor in University of Sfax, Sfax Engineering School, Control & Energy Management Laboratory (CEMLab), Sfax, Tunisia. E-mail: n.derbel@enis.rnu.tn

This variable nature causes significant challenges for the power network in terms of generation, transmission and distribution. Therefore, in order to ensure the reliability and the stability of distributed generation systems, an energy storage systems can be integrated to smooth out the fluctuations of power by providing the power deficit or by absorbing the excess of generation [4], [5]. The use of a photovoltaic energy source associated with a pack of storage batteries seems very suitable where the solar generator is considered as primary source of energy, while the storage element is used as a backup generator as shown in Fig.1.

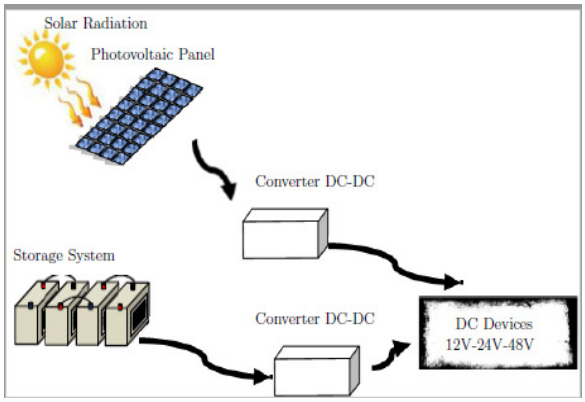

Fig.1: General diagram of a stand-alone PV installation

DC-DC power electronic converters are integrated in the adopted photovoltaic generation chain in order to transfer and converter the available power at the DC side of solar module into DC power at the loads. Two topologies have been considered. In fact, a Boost and Buck-Boost converters are needed in order to adapt the voltages of different used sources.

- DC-DC boost converter: It is inserted between the photovoltaic generator and the load. It is unidirectional in current. It has been used in PV generation system in order to set-up the terminal voltage of a PV panel to the desired voltage level at the load input. It is controlled by a PWM signal in order to perform the tracking of the optimal operating point of the PV array ensuring the maximum power generation under variations of climatic work conditions. The method of controlling converters dedicated to PV systems is called MPPT (Maximum Power Point Tracker).
- DC-DC buck-boost converter: It is interposed between the storage system pack and the DC bus. It is reversible in current due to the bidirectional character of the storage system (charging and discharging). It operates in boost mode when storage device supplies power to the load and in Buck mode in case the energy is heated to the storage system to load it.

The sizing of an isolated electric generation system is still in the field of research given its complexity in terms of modeling, optimization, and control. Therefore, each energy generation system must contain a suitable control strategy in order to ensure a continuous supply of the power to the users, and to supervisor appropriately the variation dynamics of the energy generation elements. The Power Management System (PMS) has a primordial role to control the power flow and to coordinate optimally between different components of the photovoltaic system. Thus, the control schemes associated to each adopted converters are responsible of:

- Maximum Power Point Tracking (MPPT) control unit for the PV generator in order to put it operate usually at the optimal operating point under variation of climatic conditions.

In the literature, several researchers have been focused their studies on the MPPT control issue, where the main interest has been the improvement of solar panels efficiency despite the variations of the weather conditions, such as the Perturb and Observe method, the Hill-Climbing method, sliding mode, Fuzzy logic, Artificial Neural Networks, and other improved techniques. In [6], an incremental conductance method has been used to determine periodically the MPPT, in which, based on the PV panels current and the voltage data, the instantaneous conductance has been compared with the incremental conductance. Hong. [7] has proposed a wilcoxon radial basis function network associated with an online learning process for an accurate MPPT control. A general regression of Artificial neural networks using an improved PSO algorithm is presented in [8] for the MPPT control of PV panel. In [8], a neuron network with an online training Back Propagation (BP) method is presented as a MPPT controller for a PV panel.

- Stabilization of the DC link voltage regardless the changing of operating conditions.
- Controlling the state of charge and the power flow of storage device. Many research studies have been developed on photovoltaic systems addressing the issues of complex energy supervision and power quality improvement. [9] have been presented an interested study on an energy management system of grid connected hybrid PV/battery/ultra capacitor system. A power management strategy for a PV/wind/FC/electrolyze system has been achieved in [10]. Because of the poor adaptability and instability of the standard control strategies under changing operating conditions, an important number of intensive research works have been examined and used more advanced and adaptive control techniques such as the Artificial Intelligence (AI) techniques (Fuzzy Logic (FL), Artificial Neural Networks (ANNs), and Adaptive Neuro-Fuzzy Inference Systems (ANFIS)).

In this paper, an investigation on the control structure of a PV panels, lead acid batteries is carried out. In fact, an intelligent control strategy has been developed in order to supervisor the DC-DC converters of a photovoltaic chain. Therefore, an Elman Neural Network has been applied in order to perform and control the MPPT of a PV source. Then, a study of an optimal controller for DC-DC converter interfacing storage elements based on Fuzzy logic approach have been examined. Therefore, this paper is organized as follows. The third section presents the mathematical modeling of different element of the studied energy generation system with a description of the methodology of the proposed power control strategy. Simulation results developed on the matlab/simulink environment are discussed in the fourth section. And, finally, the last section outlines the conclusion.

2. Notation

The notation used throughout the paper is stated below.

Indexes:

Ipv	output current of the PV module (A)
Vpv	output voltage of the PV module (V)
Is	reverse saturation current (A)

Constants:

η	diode ideality factor
T	temperature of the module [K]
q	electron charge [$q = 1.610^{-19}C$]

K boltzman constant $[K = 1.3810^{-23} J/K]$
Tref reference temperature $[T = 25℃]$
Gref reference irradiation $[G = 1000 W/m^2]$

3. Structure of the stand-alone photovoltaic system

Figure.2 shows the structure of the proposed stand-alone photovoltaic system which consist of a 50W PV generator, a DC-DC converters and a pack of a lead acid battery storage system of 24V, 1.2Ah. A voltage control loop has been used to control the PV- boost converter in order to reach the maximum PV generation point.

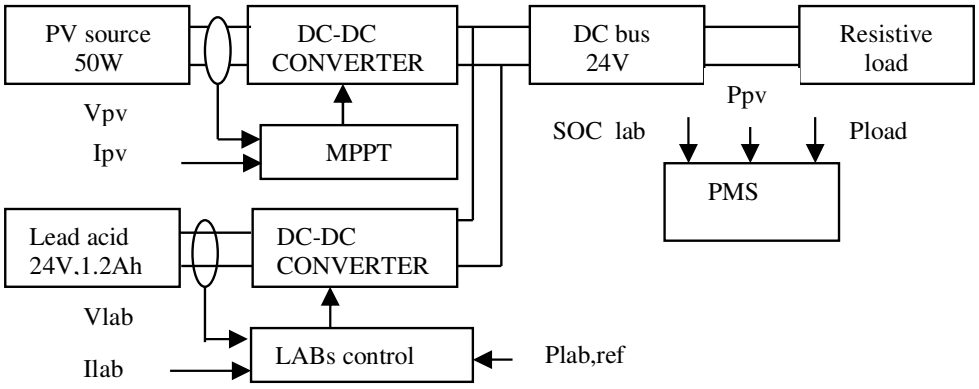

Fig.2: Overall scheme of the (PV/LAB) energy generation unit

3.1. Modeling of PV generator

The PV generator panel is defined as a panel composed by a number of PV cells connected in parallel and in series in order to obtain the desired power. It converts the photon energy into the electrical energy through the photovoltaic effect. In order to extract the actual electrical characteristic (I–V) and to exploit the influence of the temperature and the irradiation on the performance of photovoltaic generators, the modeling of solar module is essential. To build the simulation model of the adopted module of 50W, we proceed to develop a model of a cell and we associate 36 cells in series. Due to its simplicity and its ability to be emulate correctly the nonlinear behavior of a PV source, the single-diode equivalent electric circuit has been adopted in several studies and provides sufficient accuracy for many applications. It consists of a current source which generates the photocurrent I_{ph} in parallel with a single diode crossed by a current I_d, a parallel resistance R_{sh}, and a series resistance R_s. The parallel resistance R_{sh} generates the leakage current and reflects the current losses in the impurities of the structure of the cell. The configuration of the equivalent electric model is indicated in figure.3

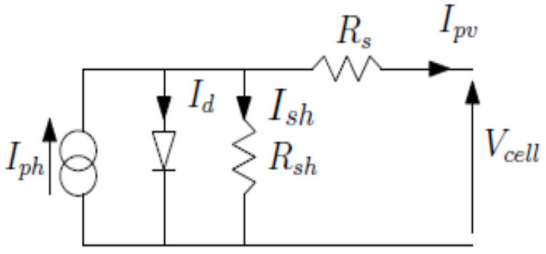

Fig.3 : The single- diode electric circuit of PV cell

The generated current Ipv of a PV cell is expressed according to the following equations:

$$Ipv = Iph - Id - Ish \quad (1)$$

$$= Iph - Is\left(exp\left(\frac{Vcell + Rs\,I}{\eta\,Vi}\right) - 1\right) - \frac{Vcell + RsI}{Rsh} \quad (2)$$

Where, $V_i = KT/q$

The electrical specifications of the proposed PV generator to be studied in this paper provided by the manufacturer in the standard test conditions STC (Tref , Gref) are summarized in table.1.

Table 1: Electrical specifications of PV module

Electrical quantities	*Value*
Voltage at maximum point (Vm,ref)	19.33V
Current at maximum point (Im,ref)	2.76A
Power at maximum point (Pm,ref)	50W
Open circuit voltage (Voc,ref)	22.93V
Short circuit current (Vsc,ref)	2.944A

3.2. DC-DC boost convereter modeling

The DC-DC boost converter has been used in PV generation system in order to set-up the terminal voltage of a PV panel to the desired voltage level at the pack of storage device input. It is controlled by a PWM signal. Figure.4 shows the electrical diagram of the studied Boost topology.

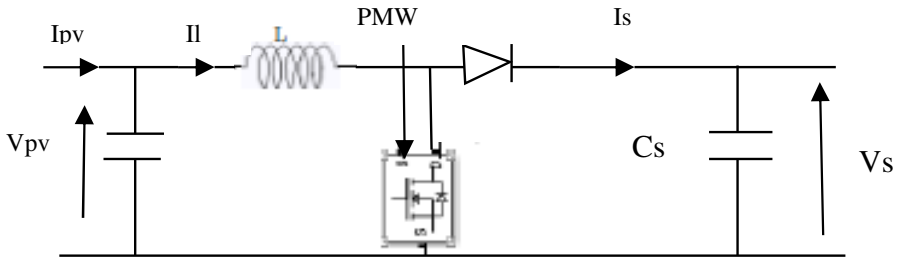

Fig.4 : Electrical structure of a boost converter

The output of the boost converter is calculated as:

$$Vs = Vpv/(1 - \alpha) \quad (3)$$

3.3. Conception of the MPPT command

This part is devoted to the analysis and synthesis of the integrated MPPT control strategy in the photovoltaic conversion chain allowing a rigorous control of the duty cycle α of the converter. The Boost control consists on the variation of the static converter duty

cycle α in order to switch the system operating point to the MPPT point and thereby extract the maximum power that the PV system can provide.

The idea is to measure the values of voltage V_{pv} and I_{pv} at time t and Δt. These measurements make it possible to decode the direction of variation of the voltage V_{pv} by increasing, maintaining, or decreasing the duty cycle α.

Perturb and observation strategy (P&O) is a widely used approach in photovoltaic applications for the search of the maximum power point. On account of improving the dynamic performances of this algorithm, a neural network has been proposed. Recently, a great interest has been given for online-trained neural network based MPPT controllers, thanks to their advantages of ability to handle the nonlinearities, and adaptability.

In this paper, an Elman Neural Network ENN algorithm has been proposed in order to determine the PV voltage reference V_{pv},ref which corresponds to the optimum operating point of the PV generator.

The adapted controller based on the ENN technique, has been established relying on the standard principle of the P&O method which consists to calculate at each iteration the PV output power P_{pv} (k) and to compare it with the previous one P_{pv} (k-1), and according to the sign of the power perturbation ΔP_{pv}pv, the V_{pv} will be perturbed. The observation and the perturbation mechanism persist until the reaching of the accurate operating point. The ENN control objective is to improve the tracking performance of P&O in term of the power fluctuations, and the convergence speed. The structure of the adopted ENN algorithm is shown in figure.5.

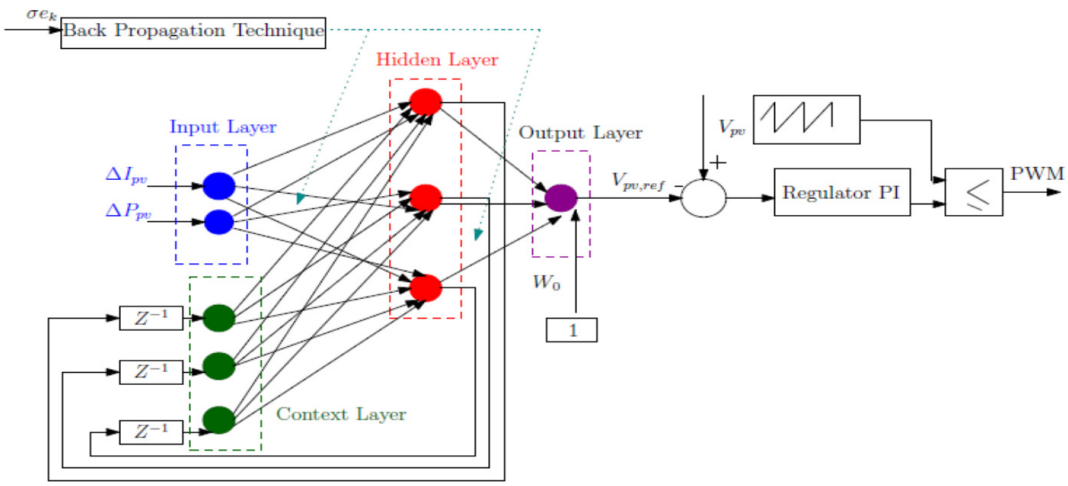

Fig.5: The structure of the adopted ENN control strategy

The ENN is a dynamic recursive artificial neural network which consists of four layers: The input layer (IL), the hidden layer (HL), the context layer (CL), and the output layer (OL).

The inputs of the ENN are the variations of the PV output current and power, $\Delta Ipv = Ipv(k) - Ipv(k-1)$, $\Delta Ppv = Ppv(k) - Ppv(k-1)$, respectively. Whereas the output is the PV voltage reference V_{pv},ref. In order to generate the PWM signal of the converter,

the error between the reference and the measured voltage will be regulated using a PI regulator in order to generate the PWM control signal of the boost converter.

A back-propagation algorithm (BP) has been adopted for the online learning of the MPPT algorithm in order to update weights of each layer.

The main role of each layer in the adopted ENN algorithm has been described by the following equations:

- Two nodes in the input layer $\left(X_i^{\,1}\right)$transmit the input signals to the hidden layer.

$$\begin{cases} X_i^{(1)}(k) = S_i^{(1)}\left(\eta_i^{(1)}\right) = \eta_i^{(1)}(k) = I_i(k), i = 1,2 \\ X_1^{(1)}(k) = \Delta P_p(k) \\ X_2^{(1)}(k) = \Delta I_p(k) \end{cases} \quad (4)$$

Where, $X_i^{(1)}$, $S_i^{(1)}$, $\eta_i^{(1)}$, and I_i present the output, the activation function, the activation level, and the input of each neuron i of the IL.

- Three nodes has been used in the hidden layer $\left(X_j^{\,2}\right)$. The output of each node is calculated as follows:

$$\begin{cases} X_j^{(2)}(k) = S_j^{(2)}\left(\eta_j^{(2)}(k)\right) \\ = S_j^{(2)}\left(\sum_i X_r^{(3)}(k) + \sum_i W_{ij} X_i^{(1)}(k)\right) \\ j = r = 1,2,3 \end{cases} \quad (5)$$

Where $X_j^{(2)}$, $S_j^{(2)}$, and $\eta_j^{(2)}$ present the output, the activation function, and the activation level of each neuron j of the HL, respectively. W_{ij} is the weight between the i-th node of the IL and j-th node of the HL, $X_r^{(3)}(k)$ is the output of the r nodes of the CL.
For the hidden layer, a tangent-sigmoid activation function has been applied.

$$\begin{cases} X_j^{(2)}(\mathrm{k}) = \dfrac{2}{\left(1+e^{-\eta_j^{(2)}}\right)} - 1 \\ X'^{(2)}_j\left(\eta_j^{(2)}\right) = \frac{1}{2}\left(1 + X_j^{(2)^2}\right) \end{cases} \quad (6)$$

- Three neurons have been used for the CL. The input of each one is the previous output of the HL.

$$X_r^{(3)}(k) = X_j^{(2)}(k-1) \quad (7)$$

- The output of the adopted ENN is expressed as follows:

$$\begin{cases} X^{(4)}(\mathrm{k}) = S^{(4)}(\eta^{(4)}(\mathrm{k})) \\ = S^{(4)}\left(W_{0+}\ \sum_j W_0 X_j{}^{(2)}(k)\right) = V_{pv,ref} \end{cases} \tag{8}$$

$S^{(4)}$ is the activation function of the OL. W_j is the synaptic weight that connect the j-th node of the HL into the OL. $W_0$is the bias weight of the output node. $S^{(4)}$ presents the sigmoid transfer function of the output node that is calculated as follows:

$$\begin{cases} X^{(4)}(\mathrm{k}) = \frac{1}{\left(1+e^{-\beta\eta^{(4)}}\right)} \\ X'^{(4)}(k) = \frac{\beta e^{-\beta\eta^{(4)}}}{\left(1+e^{-\beta\eta^{(4)}}\right)^2} \end{cases} \tag{9}$$

β is a positive constant.

The adaptation laws of the ENN weights using descent gradient rule are given as follows:

$$\begin{cases} W_{ij}(k+1) = W_{ij}(k) - \mu\frac{\delta\sigma e(k)}{W_{ij}} + \alpha\left(W_{ij}(k) - W_{ij}(k-1)\right) \\ W_j(k+1) = W_j(k) - \mu\frac{\delta\sigma e(k)}{W_j} + \alpha\left(W_j(k) - W_j(k-1)\right) \\ W_0(k+1) = W_0(k) - \mu\frac{\delta\sigma e(k)}{W_0} + \alpha\left(W_0(k) - W_0(k-1)\right) \end{cases} \tag{10}$$

Where, μ presents the learning rate of the ENN layers. μ is an important parameter which affects the convergence speed of the learning algorithm. The choice of a large learning factor can accelerate the convergence speed, but, in other hand, it can make the system more sensible with the presence of perturbation. To deal with this problem, an adaptive learning rate has been adopted for the improvement of the dynamic performance of the ENN controller algorithm.

α is the momentum factor. The formula of the adaptive learning coefficient μ is calculated as follows:

$$\mu(k) = \left[\frac{\mu_{max}-\mu_{min}}{2}\left(\frac{1}{1+e^{-\beta\gamma_k}} + 1\right) + \mu_{min}\right] \tag{11}$$

Where, μ_{max} and μ_{min} are the maximum and minimum learning rates.
$\gamma k = (Wc/(s + Wc\ ))\ \delta e\ (k)$ in which Wc is the cut off frequency of a low pass filter.
The auto-adaptation of the learning rate during the training process eliminates the power

oscillations and the static error and permits a rapid convergence speed of the back propagation algorithm.

Under given climatic conditions, the slope (dPpv/dVpv) of the PV system is close to zero at the maximum power point. Therefore, the objective function of the adapted neural MPPT controller has been determined as the quadrature error surface.

$$\begin{cases} \delta e(k) = \frac{e_s(k)^2}{2} = \left(\frac{(e_p(k)+C_1 e_p(k-1))^2}{2}\right) \\ e_p(k) = \frac{P_{pv}(k)-P_{pv}(k-1)}{V_{pv}-V_{pv}(k-1)} \end{cases} \quad (12)$$

C_1 is a positive constant. This choice of δe(k) aims to improve the characteristic of the proposed ENN-MPPT controller by maintaining the error function δe(k) equal to zero. During the operation of the system, the weights of the ENN are updated using equations.13:

$$\begin{aligned} W_{ij}(k+1) &= W_{ij}(k) - \mu e_s(k)\beta W_j X^{(4)}\left(1 - X^{(4)}\right) + \alpha\left(W_{ij}(k) - W_{ij}(k-1)\right) \\ W_j(k+1) &= W_j(k) - \mu e_s(k)\beta W_j X^{(4)}\left(1 - X_j^{(2)}\right) + \alpha\left(W_j(k) - W_j(k-1)\right) \\ W_0(k+1) &= W_0(k) - \mu e_s(k)\beta W_j X^{(4)}\left(1 - X^{(4)}\right) + \alpha\left(W_j(k) - W_j(k-1)\right) \end{aligned} \quad (13)$$

3.4. Modeling of storage system

In the PV adopted structure, a pack of 4 lead acid batteries of 6V,1.2Ah has been used as an auxiliary buck up source for the PV power generation system. In this work, the thevenin model has been adopted as shown by figure.6. The thevenin model is made up of a voltage source V_{oc} an internal resistance R_0 and one RC parallel capacitance and resistance. I denotes the load current, v indicates the battery terminal voltage. V_{oc} describes the open circuit voltage. The ohmic resistance R_0 reflects the electrical conductivity between the electrodes, the separator and the electrolyte. R_1 and $C_1$are the charge transfer resistance and the double layer capacitance between the electrolyte and the electrode, respectively. $I_1$is used to express the current which flows through R_1. V_1 and V_0 are the voltage of the resistor-capacitor RC link, and voltage of R_0, respectively.

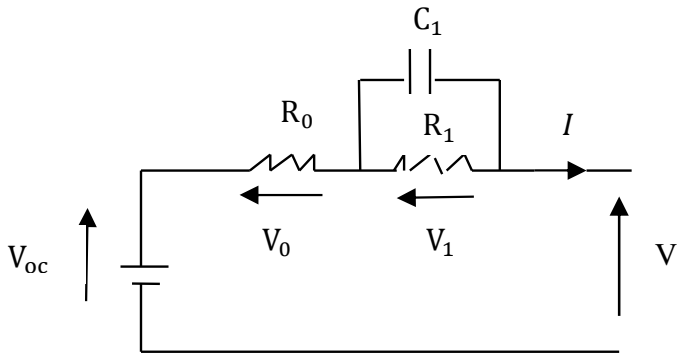

Fig.6 : Thevenin electric equivalent circuit model

The used simulation model calculates the actual voltage and state of charge according to the following equations:

$$\begin{cases} V(t) = V_{oc} - R_1 I_1 - R_0 I \\ I_1 = \frac{1}{R_1 C_1}(I - I_1) \\ \dot{V}_1 = -\frac{1}{R_1 C_1} V_1 + \frac{1}{C_1} I \\ soc = 100 * \left(1 + \frac{\int I\, dt}{Q}\right) \end{cases} \quad (14)$$

Where $V(t)$ is the actual terminal battery voltage (V), I is the battery current (A), SOC is the actual state of charge of the battery, Q is the nominal battery capacity (Ah), $\int I\, dt$ is the actual battery capacity (Ah). The battery parameters have been calculated using genetic algorithm (GA).

3.5. DC-DC buck-boost converter modeling

The topology of the adopted buck boost converter consists of two power switching elements that permits the bidirectional spread of the electrical energy. Figure.7 shows the structure of the DC-DC Buck-Boost converter.

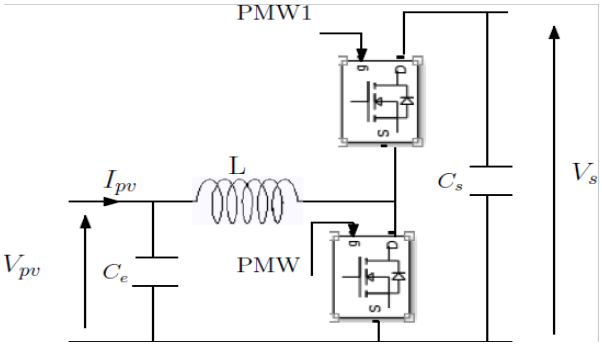

Fig.7 : Electrical structure of a buck-boost converter

The output of the buck-boost converter is calculated as follows:

$$V_s = \frac{\alpha}{1-\alpha} V_{pv} \quad (15)$$

3.6. Control of the DC-DC buck-boost converter

The performance of LAB has been controlled through conventional current control loops, in which the power reference are provided from a power management system PMS. The control structure adopted for the bidirectional converter of LAB is schematised by figure.8. The LAB's current reference is calculated through the LAB's power controller.

Then, a PI controller based on a Fuzzy Gain Tuner FGT is provided to regulate the measured LAB's current to follow the reference signal. Then, the output duty ratio is developed to generate the appropriate switching pulses for the bidirectional converter. The suggested FGT-PI strategy for the LAB's current controller has two inputs (the current error e_{ILab}, and the derivative of the current error Δe_{ILab}) and two outputs which are the updated PI parameters (the proportional and integral gains K_i and K_p).

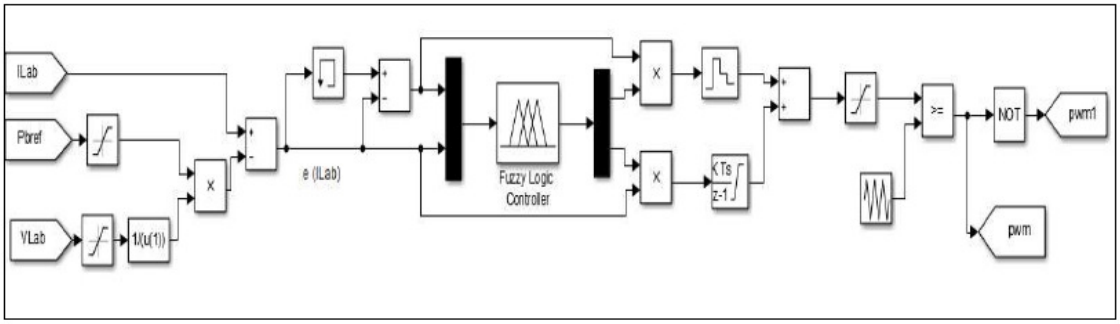

Fig.8 : Control scheme of the buck boost converter of the (PV/LAB) system

The membership functions assigned to the input and output variables of FGT of LAB's current controller are presented in Fig.9 and Fig.10. To characterize the inputs, triangular Membership Functions are selected [(Negative Large NL), (Negative Medium NM), (Negative Small NS), (Zero Z), (Positive Small PS), (Positive Medium PM), and (Positive PL large)]. Moreover, For the FGT outputs four triangular Membership Functions are developed (Small S), (Medium M), (Medium Large ML), and (Large L).

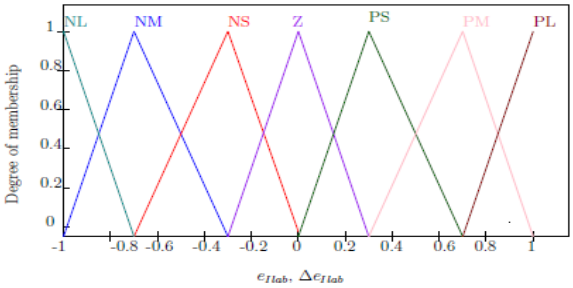

Fig.9 : Membership functions assigned to the input variables (e_{ILab},Δe_{eILab})

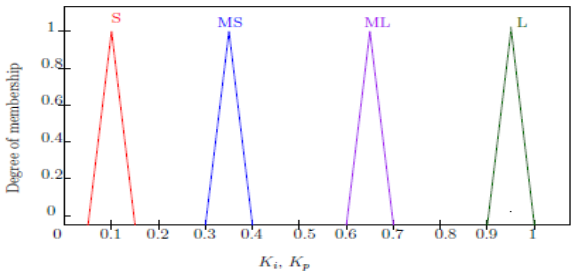

Fig.10 : Membership functions assigned to the output variables (K_i, K_p)

The FGT rules are established in table.2 and table.3.

Table 2: Rules for tuning the gain K_p of FGT of Lab controller

e_{ILab}	Δe_{ILab}						
	NL	NM	NS	Z	PS	PM	PL
NL	L	L	L	L	L	L	L
NM	ML	ML	ML	MS	ML	ML	ML
NS	ML	MS	MS	MS	MS	MS	ML
Z	MS	MS	S	S	S	MS	MS
PS	ML	MS	MS	MS	MS	MS	ML
PM	ML	ML	ML	MS	ML	ML	ML
PL	L	ML	L	L	L	L	L

Table 3: Rules for tuning the gain K_i of FGT of Lab controller

e_{ILab}	Δe_{ILab}						
	NL	NM	NS	Z	PS	PM	PL
NL	S	ML	ML	ML	ML	ML	S
NM	ML	MS	MS	ML	MS	MS	ML
NS	ML	MS	L	L	L	ML	ML
Z	L	L	L	L	L	L	L
PS	ML	ML	L	L	L	ML	ML
PM	ML	MS	MS	ML	MS	MS	ML
PL	L	ML	ML	ML	ML	ML	L

A power management system has been provided to supervisor the power flow, and to calculate the power's LAB reference $P_{Lab,ref}$ in such away that the load power requirements are satisfied. According to the power load, the availability of the PV power, and the state of charge of LABs, the PMS controls the bidirectional DC-DC converter of LAB and determines the modes of operation (charge or discharge). Figure.11 shows the flowchart of the adopted PMS.

The PV source is considered as the principal energy source, whereas, the pack of lead acid batteries is used as complementary power sources. The control process starts by comparing the generated PV power (P_{pv}) and the load power (P_{Load}). The charge-discharge process of the battery pack is controlled in order to maintain the SOC range at reasonable level, and so to increase its lifetime.

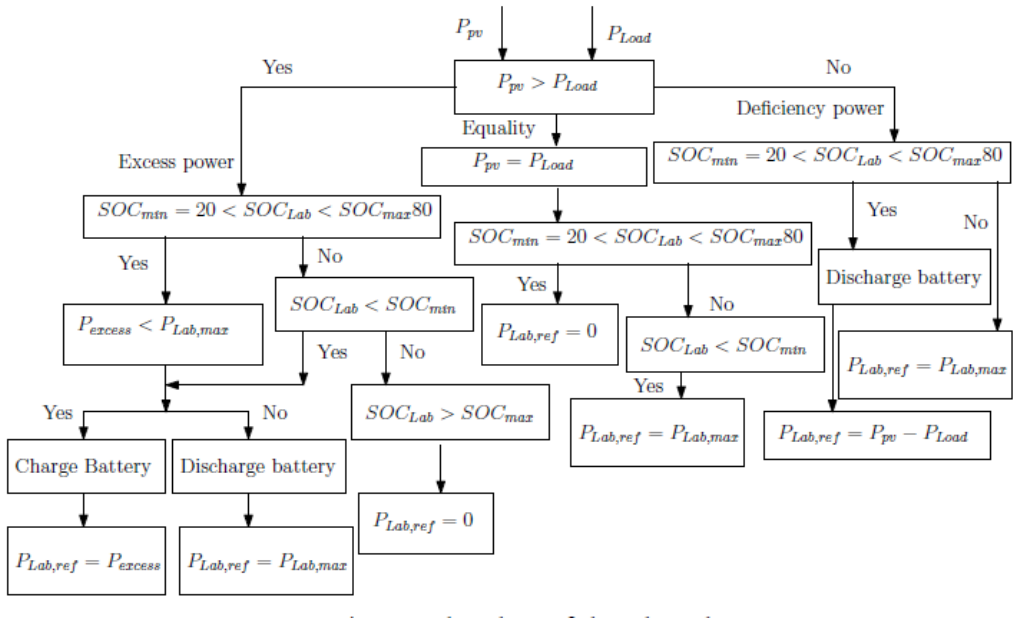

Fig. 11 : Flowchart of the adopted power management system PMS

4. Simulation results

The photovoltaic conversion chain is simulated with a resistive load connected to the output of the value converter R_s= 16.8 Ω

In order to validate the accuracy of the adopted ENN control strategy, simulation tests under various climatic conditions has been performed:

- In the first test, climatic conditions are constants: (the temperature $T = 25℃$, the irradiation $G = 1000\,W/m^2$), with a resistive load R_s= 16.8 Ω . As depicted in figure.14, the optimal operating point of the PV panel has been quickly reached using the adopted ENN-MPPT controller after a short time of 0.0036s whereas using P&O, the response time is around 0.07s .

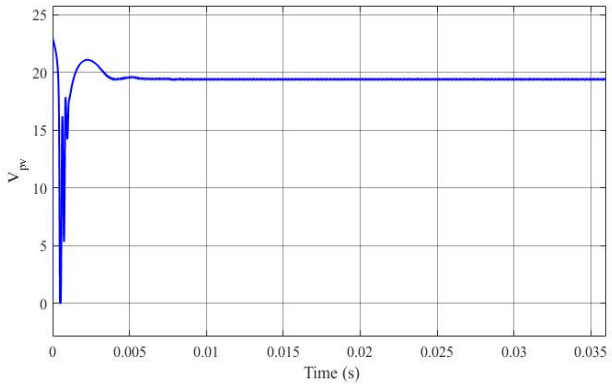

Fig.12: PV voltage with constant climatic conditions

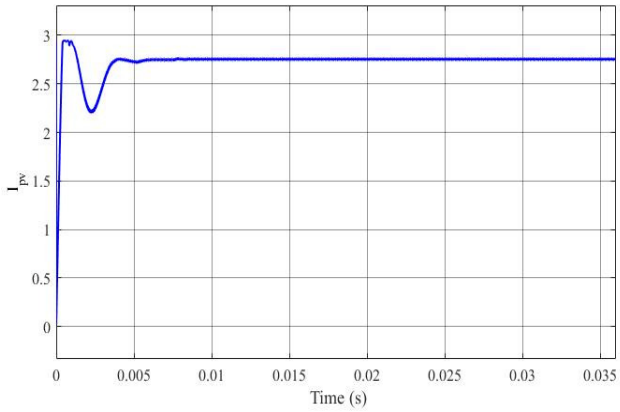

Fig.13: PV current with constant weather conditions

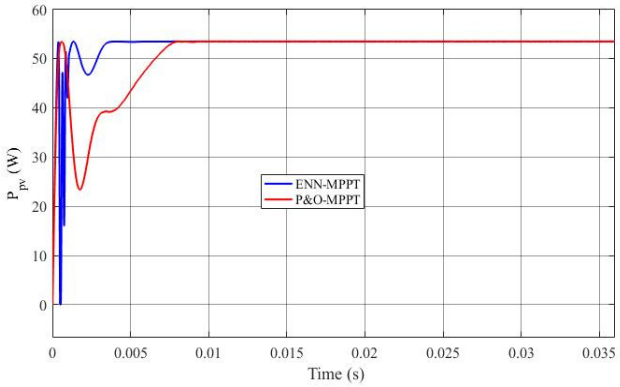

Fig.14: PV power with unchanged climatic conditions

- In the second test, the temperature is constant ($T = 25℃$), while the radiation level have been varied as presented in figure.15. It is obvious from figure.16, and figure.18, that despite the fluctuation of the irradiance, the proposed ENN-MPPT controller acts correctly in order to ensure the best tracking performance. Using the adopted ENN, a good steady state characteristic is obtained in comparison with the P&O method.

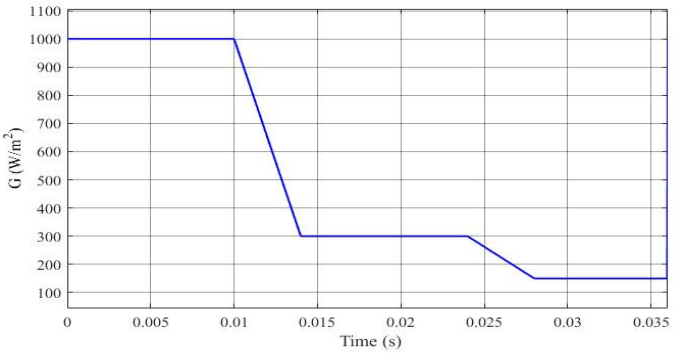

Fig.15 : Variation of the irradiance

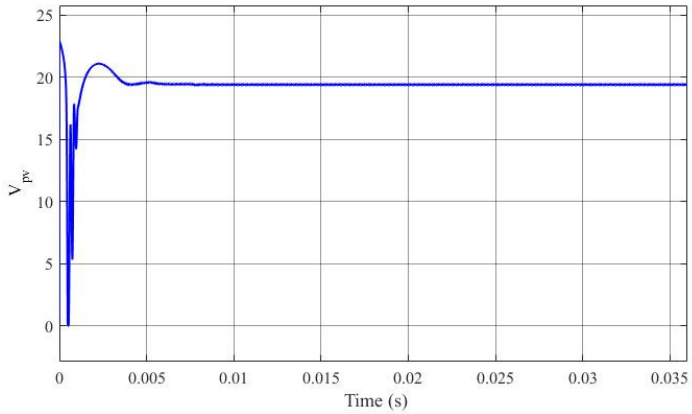

Fig.16 : PV voltage with constant temperature and with variations of the irradiance

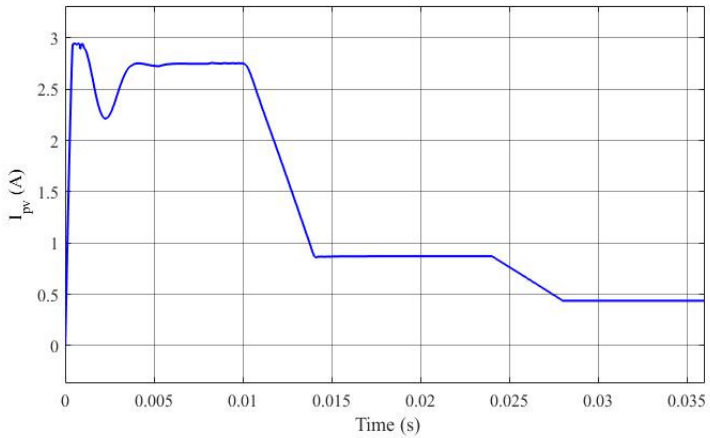

Fig.17 : PV current with unchanged temperature and with variations of the irradiance

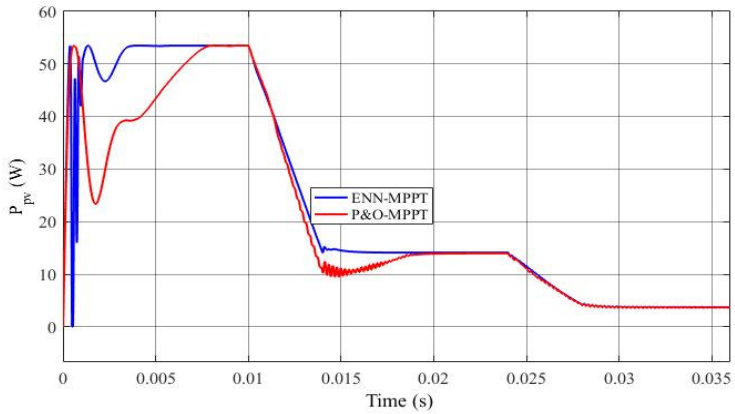

Fig.18 : PV power with constant temperature and with variations of the irradiance

- In the third test, the temperature varies from 10 ℃ to 50 ℃ then decreases to 5℃ at a constant irradiance $G = 1000W/m^2$, as illustrated in figure.19. Figure.20, figure.21, and figure.22 show respectively the solar panel voltage, the PV current, and the

PV power with constant irradiance and with temperature variations. Figure.22 presents the superiority of the proposed ENN-MPPT tracker than the P&O technique.

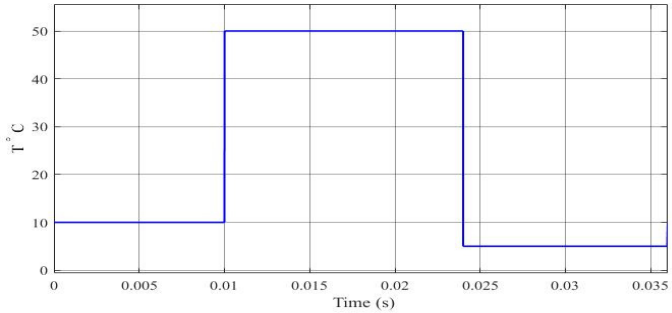

Fig.19 : Variation of temperature

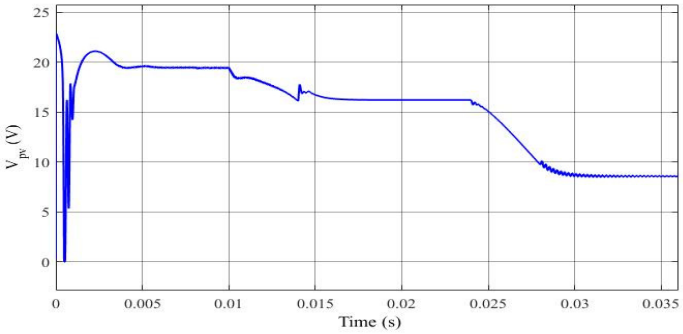

Fig.20 : PV voltage with constant irradiance and with temperature variations

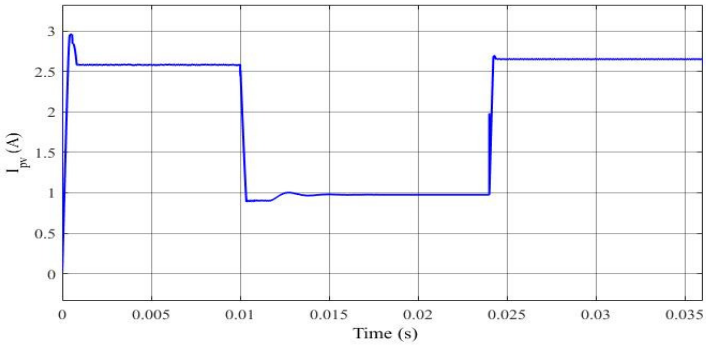

Fig.21 : PV current with constant irradiance and with temperature variations

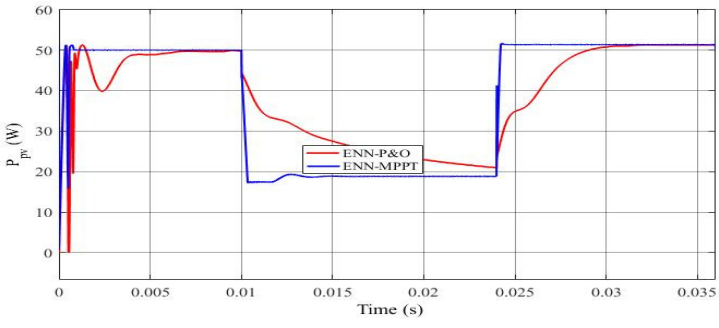

Fig.22 : PV power with constant irradiance and with temperature variations

In order to validate the effectiveness of the adopted FL control method, simulation tests under different climatic conditions and variable load demand are performed. The secure range of the state of charge of the battery is set between 20% and 80%. The following simulation tests have been performed:

- The power generated by the PV is over the load demand (P_{PV}>P_{Load} and the SOC_{min}<SOC=45<SOC_{min}). As depicted in figure.23, the bus voltage is perfectly stable at the reference value 24V with the exception of overtaking shown during the first seconds, which is acceptable during the transient regime. On the other hand, it is obvious from figure.24 and figure.25 that the power management system determines correctly the power reference of the battery pack according to the available PV power and Load power. In this case, the excess of the power is used to charge the battery as shown by figure.26.

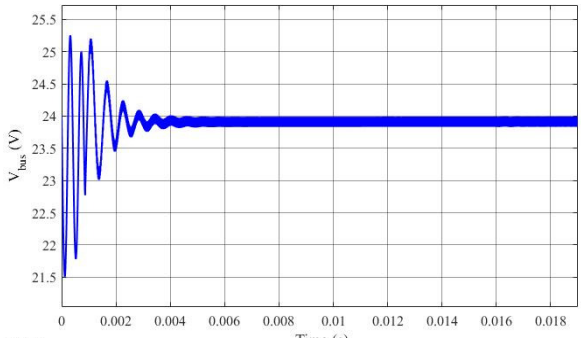

Fig.23 : DC-Link voltage V_{Bus}

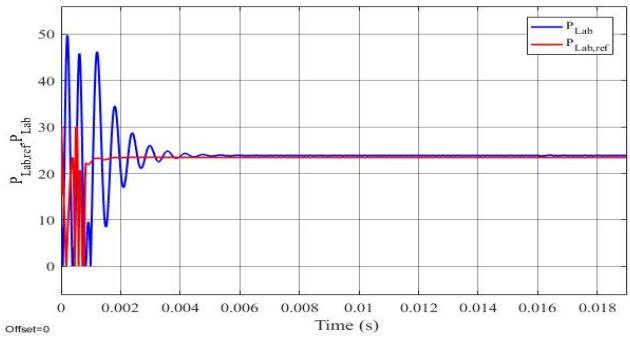

Fig.24 : Battery power

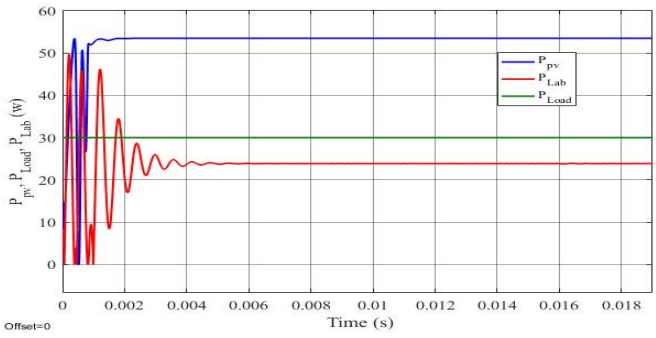

Fig.25: Active power of the PV, the battery, and the load

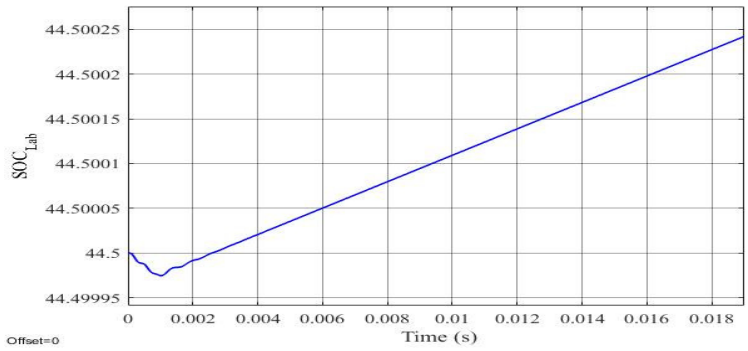

Fig.26 : State of charge of the battery

- The power generated by the PV is over the load demand ($\boldsymbol{P_{pv} > P_{Load}}$ and the SOC> $\boldsymbol{SOC_{max}}$). In this case, the battery stops to charge avoiding the overcharging as shown by figure.27.

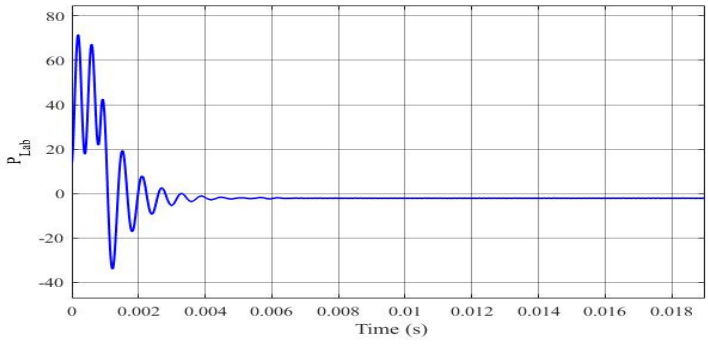

Fig.27 : Battery power P_{Lab} for SOC> SOC_{max}

- The power demand surpasses the rated power of the generator unit $\boldsymbol{P_{Load}}$>$\boldsymbol{P_{pv}}$, and the $\boldsymbol{SOC_{min}}$<SOC=45<$\boldsymbol{SOC_{max}}$. In this case, the state of charge of the battery pack is in within allowable level, so it delivers the power deficit. Figure.29 shows the SOC of the battery pack. From figure.30. and figure.31, we can constat that the power supervisor sets properly the power set points for the storage device.

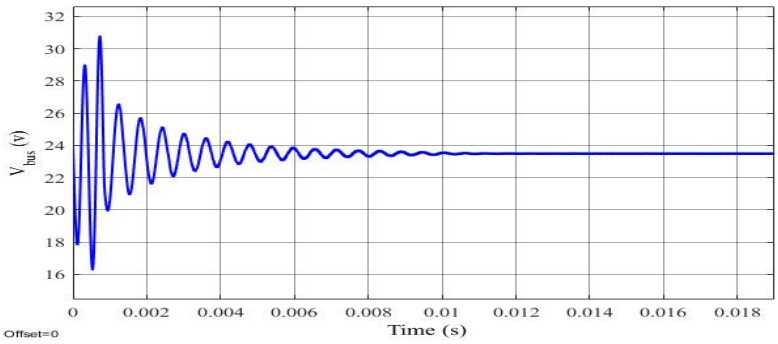

Fig.28 : Bus voltage V_{Bus} for P_{Load}>P_{pv}

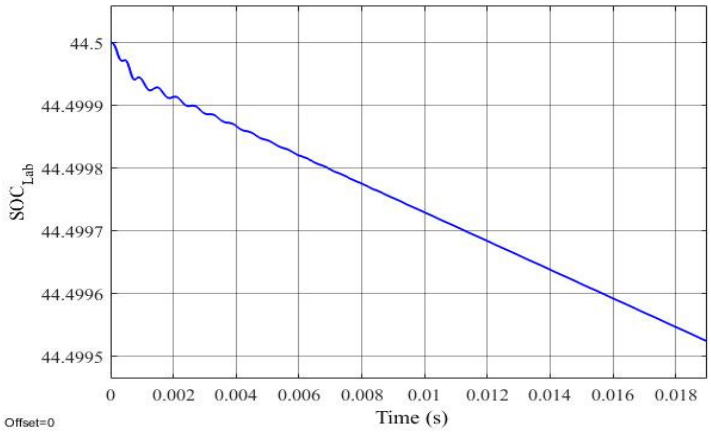

Fig.29 : State of charge SOC_{Lab} for P_{Load}>P_{pv}

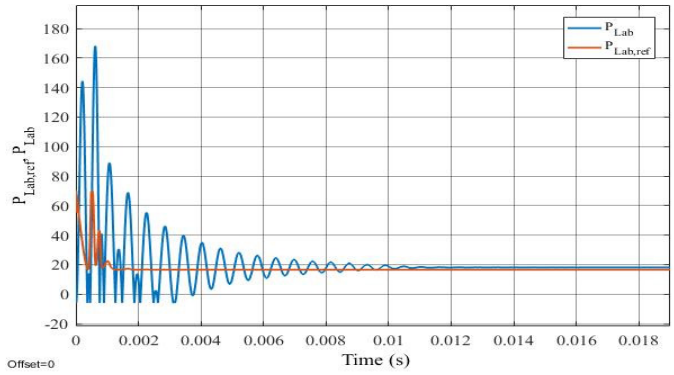

Fig. 30 : Power of battery for P_{Load}>P_{pv}

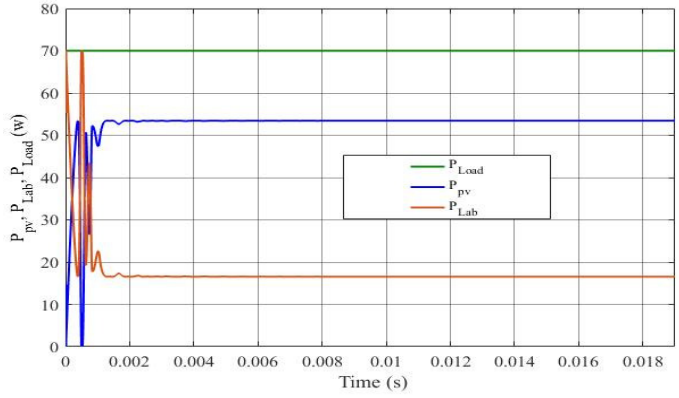

Fig.31 : Active power of different elements of the PV unit for P_{Load}>P_{pv}

5. Conclusion

In this paper, an intelligent control strategy for a stand-alone photovoltaic system has been evaluated in the Matlab/Simulink environment. Intelligent local controllers for the DC-DC converters based on the ANN, and FLC have been adopted and implemented.

Thus, a control power supervisor has been designed to well manage the power sharing between the different components of the PV chain. The obtained simulation results show the validity and the effectiveness of the proposed control methods under variable operating work conditions. The adopted ENN-MPPT demonstrates a good tracking performance in comparison with the conventional P\&O algorithm.

References

[1] Mita Bhattacharyaa, Sudharshan Reddy Paramatib, Ilhan Ozturkc, Sankar Bhattacharya, The effect of renewable energy consumption on economic growth, *Applied Energy*, pp.733-41, 2016.

[2] Viet T. Tran, Danny Sutanto ,Kashem M. Muttaqi, Advantage of time-of-use electricity pricing, 2017.

[3] International Energy Agency. IEA. World Energy Outlook 2013, *Global Energy Trends, Renewable Energy Outlook-IEA*,2013.

[4] Witold Maranda, Capacity Degradation of Lead-acid Batteries Under Variable-depth Cycling Operation in Photovoltaic System, *the 22nd International Mixed Design of Integrated Circuits and Systems*, 2015, Poland .

[5] Grigorios L, Kyriakopoulos, Garyfallos Arabatzis, Electrical energy storage systems in electricity generation : *Energy policies, innovative technologies, and regulatory regimes, Renewable and Sustainable Energy Reviews*, Vol. 56, pp.1044-1067, April 2016.

[6] .H. Hussein, I. Muta, T. Hoshino, M. Osakada, Maximum photovoltaic power tracking: an algorithm for rapidly changing atmospheric conditions, 1995.

[7] Hong CM, Ou TC, Lu KH. Development of intelligent MPPT (maximum power point tracking) control for a grid-connected hybrid power generation system. *Energy,* 2013.

[8] Garca-Trivino P, Gil-Mena AJ, Power control based on particle swarm optimization of grid-connected inverter for hybrid renewable energy system. *Energy Convers Manag,* 2015.

[9] Choudar A, Boukhetala D, Barkat S, Brucker JM, A local energy management of a hybrid PV-storage based distributed generation for microgrids, *Energy Convers Manag,* 2015.

[10] N. Chettibi, A. Mellit, FPGA-based real time simulation and control of grid-connected photovoltaic systems, *Simulation Modelling Practice and Theory*, 2014.

[11] Jihen Loukil, Ferdaous Masmoudi, Nabil Derbel. State of charge estimation of lead acid battery using an ARX model and an Extented kalman filter, *International Seminar on Applied Research and Technology Transfer (CRATT'17)*, Tunisia, April (2017).

[12] Jihen Loukil, Ferdaous Masmoudi, Nabil Derbel. Elman neural network control strategy for a photovoltaic system, *International Conference on Recent Advances in Electrical Systems (ICRAES'18)*, Hammamet, Tunisia , December (2018).

[13] N. Chettibi, A. Mellit, Intelligent control strategy for a grid connected PV/SOFC/BESS energy generation system, *Energy*, 2018.

[14] Zhao ZY, Tomizuka M, Isaka S, Fuzzy gain scheduling of PID controllers, *IEEE Trans Syst Man,* 1993.

[15] Kofinas P, Dounis AI, Papadakis G, Assimakopoulos MN, An Intelligent MPPT controller based on direct neural control for partially shaded PV system, *Energy Build* , 2015.

[16] Ahmed J, Salam Z, A critical evaluation on maximum power point tracking methods for partial shading in PV systems, *Renew Sustain Energy*, 2015.

[17] Hong CM, Ou TC, Lu KH, Development of intelligent MPPT (maximum power point tracking) control for a grid-connected hybrid power generation system, *Energy* 2013.

[18] N. Femia, G. Petrone, G. Spagnuolo, M. Vitelli, Optimization of perturb and observe maximum power point tracking method, *IEEE Trans Power Electron*, 2005.

[19] A. Safari, S. Mekhilef, Simulation and hardware implementation of incremental conductance MPPT with direct control method using cuk converter , *IEEE Trans Industr Electron,* 2011.

[20] K.H. Hussein, I. Muta, T. Hoshino, M. Osakada, Maximum photovoltaic power tracking: an algorithm for rapidly changing atmospheric conditions*, IEE Proc Gener Transm Distrib*, 1995.

[21] E. Koutroulis, K. Kalaitzakis, N.C. Voulgaris, Development of a microcontroller-based photovoltaic MPPT control system, *IEEE Trans Power Electron*, 2001.

[22] Nandar CA, Robust PI control of smart controllable load for frequency stabilization of microgrid power system, *Renew Energy* , 2013.

[23] Hajizadeh A, Golkar MA. Intelligent robust control of hybrid distributed generation system, *Expert Syst*, 2010.

[24] Berrazouane S, Mohammedi K, Parameter optimization via cuckoo optimization algorithm of fuzzy controller for energy management of a hybrid power system, *Energy Convers Manag,* 2014.

[25] Garca Trivi, Gil Mena Llorens Iborra, Garca CA, Fernandez Ramrez , Jurado, Power control based on particle swarm optimization of grid-connected inverter for hybrid renewable energy system, *Energy Convers Manag,* 2015.

[26] Garcia P, Garcia CA, Fernandez LM, Llorens F, Jurado F, ANFIS-based control of a grid-connected hybrid system integrating renewable energies, hydrogen and batteries, 2014.